# Radiative neutrino mass model in dark non-Abelian gauge symmetry

Takaaki Nomura[1,*] and Hiroshi Okada[2,3,†]

[1]*College of Physics, Sichuan University, Chengdu 610065, China*
[2]*Asia Pacific Center for Theoretical Physics, Pohang 37673, Republic of Korea*
[3]*Department of Physics, Pohang University of Science and Technology, Pohang 37673, Republic of Korea*

(Received 22 July 2021; accepted 4 March 2022; published 11 April 2022)

We discuss a model based on the dark sector described by a non-Abelian $SU(2)_D$ gauge symmetry where we introduce $SU(2)_L \times SU(2)_D$ bidoublet vector-like leptons to generate active neutrino masses and kinetic mixing between $SU(2)_D$ and $U(1)_Y$ gauge fields at the one-loop level. After spontaneous symmetry breaking of $SU(2)_D$, we have a remnant $Z_4$ symmetry, guaranteeing the stability of dark matter candidates. We formulate the neutrino mass matrix and related lepton-flavor-violating processes and discuss dark matter physics where we estimate relic density of dark matter. We find that our model realizes a multicomponent dark matter scenario due to the $Z_4$ symmetry, and that the relic density can be explained by gauge interactions with a kinetic mixing effect.

DOI: 10.1103/PhysRevD.105.075010

## I. INTRODUCTION

A mechanism for generating neutrino masses and the existence of dark matter (DM) are key to understanding physics beyond the standard model (SM). One attractive scenario is that DM and neutrino-mass generation are induced from a dark sector described by dark gauge symmetry, under which the SM fields are singlets. Then, we would expect that the nature of the neutrino-mass generation mechanism and DM physics could be understood using dark gauge symmetry. For example, the stability of DM could be understood by using a remnant of dark gauge symmetry [1,2], and neutrino masses at tree level can be forbidden by such a symmetry.

One interesting scenario is a non-Abelian dark gauge symmetry, such as $SU(2)$, which provides a dark sector with a rich structure and the possibility of vector DM from the dark gauge sector and $Z'$ as a mediator at the same time. In fact, various approaches using a dark $SU(2)$ gauge symmetry can be found in the literature, such as a remaining $Z_{2,3,4}$ symmetry with a quadruplet (quintet) [3–9], $Z_2 \times Z_2'$ symmetry [10], a custodial symmetry [11–13], an unbroken $U(1)$ from $SU(2)$ [14–16], a model adding a hidden $U(1)_h$ [17], other DM scenarios [18–21], a model with classical scale invariance [22], baryogenesis [23], and the electroweak phase transition [24]. Here, one interesting question for the non-Abelian dark-gauge-symmetric case is how we can induce interactions among dark gauge bosons and the SM particles, since kinetic mixing is not allowed at a renormalizable level in contrast to the Abelian gauge-symmetric case. In Ref. [25], we showed that such a term at the one-loop level can generate kinetic mixing between dark $SU(2)$ and the SM $U(1)_Y$, introducing fields that have both dark $SU(2)$ and $U(1)_Y$ charges. Interestingly, when we choose such fields as vector-like leptons, they can also play a role in generating active neutrino masses at the loop level [26–28] by adding relevant dark $SU(2)$ multiplet scalar fields.

In this work, we discuss a model with non-Abelian $SU(2)_D$ gauge symmetry in which we introduce $SU(2)_L \times SU(2)_D$ bidoublet vector-like leptons. These bidoublet leptons can induce mixing among $SU(2)_D$ and $U(1)_Y$ gauge fields and play a role in generating active neutrino masses when we introduce relevant scalar $SU(2)_D$ multiplets. We also find that there is a remnant $Z_4$ symmetry after spontaneous symmetry breaking, and the stability of DM is guaranteed by this symmetry. We then formulate active neutrino masses and branching ratios (BRs) of the lepton-flavor-violating (LFV) charged lepton decay $\ell_i \to \ell_j \gamma$ in our model. In addition, the relic density of our dark matter (DM) candidate is estimated, where DM is more than one component in our scenario.

This paper is organized as follows. In Sec. II we introduce our model, and show its relevant Lagrangian and particle content. In Sec. III we discuss the phenomenology of the model, such as the neutrino masses, LFVs and DM physics. In Sec. IV we provide a summary and discussion.

*nomura@scu.edu.cn
†hiroshi.okada@apctp.org

## II. A MODEL

We consider a model based on $G_{\rm SM} \times SU(2)_D$ gauge symmetry, where $G_{\rm SM}$ represents the SM gauge symmetries and $SU(2)_D$ is the additional symmetry in our dark sector. For the fermion sector, we introduce an $SU(2)_L \times SU(2)_D$ bidoublet lepton $L'$ with $U(1)_Y$ charge $-1/2$, and an $SU(2)_D$ doublet $N$ which is a singlet under $G_{\rm SM}$. Here, three generations of these fermions are considered in our model. For the scalar sector, we introduce an $SU(2)_D$ complex quintet $\Phi$, a real triplet $\varphi$, and a complex doublet $\chi$; the SM Higgs doublet $H$ is also included. The new field content is summarized in Table I with their charge assignments. We write $L'$ and $N$ as

$$L' = \begin{pmatrix} n'_1 & n'_2 \\ e'_1 & e'_2 \end{pmatrix}, \qquad N = \begin{pmatrix} n_1 \\ n_2 \end{pmatrix}, \tag{1}$$

where indices that distinguish generations are omitted. The scalar multiplets are written as

$$\chi = \begin{pmatrix} \chi_1 \\ \chi_2 \end{pmatrix}, \qquad \varphi = \begin{pmatrix} \frac{\varphi_0}{\sqrt{2}} & \varphi_+ \\ \varphi_- & -\frac{\varphi_0}{\sqrt{2}} \end{pmatrix},$$
$$\Phi = (\,\Phi_{++} \quad \Phi_+ \quad \Phi_0 \quad \tilde{\Phi}_- \quad \tilde{\Phi}_{--}\,)^T, \tag{2}$$

where $\varphi_+ = (\varphi_-)^*$. The triplet $\varphi$ can be written as $\varphi^\alpha \sigma_\alpha/2$ ($\alpha = 1, 2, 3$), with $\sigma^\alpha$ being the Pauli matrix acting on $SU(2)_D$ representation space; thus, we redefine $\varphi_0 = \varphi^3$ and $\varphi_\pm = (\varphi^1 \mp i\varphi^2)/\sqrt{2}$. The SM Higgs field is written as

TABLE I. Charge assignment for the fields in the $SU(2)_D$ dark sector, where $\{\chi, \varphi, \Phi\}$ are scalars and $\{L', N\}$ are Dirac fermions. We introduce three generations of new fermions; we choose the number of generations to match that of the SM fermions, but we can also choose small number of generations.

| Fields | $L'$ | $N$ | $\chi$ | $\varphi$ | $\Phi$ |
|---|---|---|---|---|---|
| $SU(2)_D$ | **2** | **2** | **2** | **3** | **5** |
| $SU(2)_L$ | **2** | **1** | **1** | **1** | **1** |
| $U(1)_Y$ | $-\frac{1}{2}$ | 0 | 0 | 0 | 0 |

$$H = \begin{pmatrix} G^+ \\ \frac{1}{\sqrt{2}}(v + h + iG^0) \end{pmatrix}, \tag{3}$$

where $v \simeq 246$ GeV is the vacuum expectation value (VEV) and $G^{+(0)}$ is the Nambu-Goldstone boson absorbed by the $W^+$ ($Z$) boson.

The Lagrangian of our model is written as

$$\mathcal{L} = \mathcal{L}_{\rm SM} + \mathcal{L}_{\rm New} + V, \tag{4}$$

where $\mathcal{L}_{\rm SM}$ is the SM Lagrangian without the Higgs potential, $\mathcal{L}_{\rm New}$ includes new terms in our model, and $V$ is the scalar potential. The new terms and the potential are given such that

$$\begin{aligned}\mathcal{L}_{\rm New} = &-\frac{1}{4}\tilde{X}^{\alpha\mu\nu}\tilde{X}^\alpha_{\mu\nu} + {\rm Tr}[\bar{L}'(D_\mu\gamma^\mu - M_{L'})L'] + \bar{N}(\partial^\mu\gamma_\mu - M_N)N \\ &+ (D^\mu\chi)^\dagger(D_\mu\chi) + \frac{1}{2}{\rm Tr}[(D^\mu\varphi)^\dagger(D_\mu\varphi)] + \frac{1}{2}(D^\mu\Phi)^\dagger(D_\mu\Phi) \\ &+ f_{ia}\bar{L}^i_L L'^a_R(i\sigma_2)\chi + f'_{ia}\bar{L}^i_L L'^a_R\chi^* + g^{ab}_R\bar{L}'^a_R N^b_L\tilde{H} + g^{ab}_L\bar{L}'^a_L N^b_R\tilde{H} \\ &+ y^{ab}_{N_L}\overline{N^{ac}_L}(i\sigma_2)\varphi N^b_L + y^{ab}_{N_R}\overline{N^{ac}_R}(i\sigma_2)\varphi N^b_L + y^{ab}_D\bar{N}^a_L\varphi N^b_R + y_{ab}\bar{L}'^a\varphi L'^b,\end{aligned} \tag{5}$$

$$\begin{aligned}V = &-M^2_H H^\dagger H + M^2_\chi\chi^\dagger\chi + \frac{1}{2}M^2_\varphi{\rm Tr}[\varphi\varphi] - M^2_\Phi\Phi^\dagger\Phi + \lambda_\chi(\chi^\dagger\chi)^2 + \lambda_\varphi{\rm Tr}[\varphi\varphi]^2 + \lambda_\Phi(\Phi^\dagger\Phi)^2 \\ &+ \lambda_H(H^\dagger H)^2 + \mu_1(\Phi^\dagger\hat{\varphi}\Phi) + \mu_2(\chi(i\sigma_2)\varphi\chi + {\rm H.c.}) + \lambda_{\varphi\Phi}{\rm Tr}[\varphi\varphi](\Phi^\dagger\Phi) \\ &+ \lambda_{\varphi H}{\rm Tr}[\varphi\varphi](H^\dagger H) + \lambda_{\Phi H}(\Phi^\dagger\Phi)(H^\dagger H) + \lambda_{\chi H}(\chi^\dagger\chi)(H^\dagger H) + \lambda_{\chi\varphi}(\chi^\dagger\chi){\rm Tr}[\varphi\varphi] \\ &+ \lambda_{\chi\Phi}(\chi^\dagger\chi)(\Phi^\dagger\Phi) + \tilde{\lambda}_{\varphi\Phi}\Phi^\dagger\hat{\varphi}\,\hat{\varphi}\,\Phi,\end{aligned} \tag{6}$$

where $\tilde{X}^{\alpha\mu\nu}$ is the gauge field strength for $SU(2)_D$, with $\alpha = 1, 2, 3$ being the index of the $SU(2)_D$ adjoint representation, and $\hat{\varphi} \equiv \varphi^\alpha \mathcal{T}^{(5)}_\alpha$ is the $5 \times 5$ notation for the scalar triplet [$\mathcal{T}^{(5)}_\alpha$ is the $5 \times 5$ notation of $SU(2)_D$ generation given in the Appendix]. We assume that the Lagrangian is invariant under $\Phi \to -\Phi$ to simplify scalar potential forbidding nontrivial cubic terms such as $\Phi^3$ and $\Phi\varphi\varphi$.

### A. Scalar sector and symmetry breaking

First, we consider gauge-invariant operators in the scalar potential in terms of the components of the scalar multiplets. Quadratic terms are given by

$$\chi^\dagger\chi = \chi^*_1\chi_1 + \chi^*_2\chi_2, \tag{7}$$

$$\frac{1}{2}\mathrm{Tr}[\varphi\varphi] = \frac{1}{2}\varphi_0^2 + \varphi_+\varphi_-, \tag{8}$$

$$\Phi^\dagger\Phi = \Phi_0^2 + \Phi_{++}\Phi_{--} + \Phi_+\Phi_- + \tilde{\Phi}_{++}\tilde{\Phi}_{--} + \tilde{\Phi}_+\tilde{\Phi}_-. \tag{9}$$

Nontrivial terms in the potential are written as

$$\begin{aligned}\Phi^\dagger\hat{\varphi}\Phi = {}& \sqrt{3}\Phi_0\tilde{\Phi}_+\varphi_- + \sqrt{3}\Phi_0\Phi_-\varphi_+ + \sqrt{3}\Phi_0^*\Phi_+\varphi_- + \sqrt{3}\Phi_0^*\tilde{\Phi}_-\varphi_+ \\ & + (2\Phi_{++}\Phi_{--} + \Phi_+\Phi_- - \tilde{\Phi}_+\tilde{\Phi}_- - 2\tilde{\Phi}_{++}\tilde{\Phi}_{--})\varphi_0 \\ & + \sqrt{2}\Phi_{--}\Phi_+\varphi_+ + \sqrt{2}\tilde{\Phi}_{--}\tilde{\Phi}_+\varphi_+ + \sqrt{2}\Phi_{++}\Phi_-\varphi_- + \sqrt{2}\tilde{\Phi}_{++}\tilde{\Phi}_-\varphi_-,\end{aligned} \tag{10}$$

$$\begin{aligned}\Phi^\dagger\hat{\varphi}\,\hat{\varphi}\,\Phi = {}& \varphi_0^2(4\Phi_{++}\Phi_{--} + 4\tilde{\Phi}_{++}\tilde{\Phi}_{--} + \Phi_+\Phi_- + \tilde{\Phi}_+\tilde{\Phi}_-) \\ & + \varphi_+\varphi_-(2\Phi_{++}\Phi_{--} + 2\tilde{\Phi}_{++}\tilde{\Phi}_{--} + 5\Phi_+\Phi_- + 5\tilde{\Phi}_+\tilde{\Phi}_-) \\ & + \varphi_-^2(3\Phi_+\tilde{\Phi}_+ + \sqrt{6}\Phi_0\tilde{\Phi}_{++} + \sqrt{6}\Phi_0^*\Phi_{++}) + \varphi_+^2(3\Phi_-\tilde{\Phi}_- + \sqrt{6}\Phi_0^*\tilde{\Phi}_{--} + \sqrt{6}\Phi_0\Phi_{--}) \\ & + \sqrt{3}\varphi_0\Phi_0(\Phi_-\varphi_+ - \tilde{\Phi}_+\varphi_-) + \sqrt{3}\varphi_0\Phi_0^*(\Phi_+\varphi_- - \tilde{\Phi}_-\varphi_+) \\ & + 3\sqrt{2}\varphi_0(\Phi_{++}\Phi_-\varphi_- + \Phi_{--}\Phi_+\varphi_+ - \tilde{\Phi}_{++}\tilde{\Phi}_-\varphi_- - \tilde{\Phi}_{--}\tilde{\Phi}_+\varphi_+),\end{aligned} \tag{11}$$

$$\chi(i\sigma_2)\varphi\chi + \mathrm{H.c.} = -\sqrt{2}\varphi_0\chi_1\chi_2 + \varphi_-\chi_1\chi_1 - \varphi_+\chi_2\chi_2 + \mathrm{H.c.} \tag{12}$$

Note that the other quartet terms are trivially given by applying quadratic terms and we do not write them explicitly. We then consider VEVs of the scalar fields by the condition $\partial V/\partial\phi = 0$, where $\phi$ represents any scalar field in the model. We find that we can take VEVs of $\tilde{\Phi}_{\pm\pm}$ and $\varphi_0$ to be nonzero, and we write them as $\langle\tilde{\Phi}_{\pm\pm}\rangle \equiv v_\Phi/\sqrt{2}$ and $\langle\varphi_0\rangle \equiv v_\varphi/\sqrt{2}$. These VEVs are derived from the following conditions:

$$\begin{aligned}v_\Phi\Big(-M_\Phi^2 - \sqrt{2}\mu_1 v_\varphi + 2\tilde{\lambda}_{\varphi\Phi}v_\varphi^2 + \frac{1}{2}\lambda_{\Phi H}v^2 \\ + \frac{1}{2}\lambda_{\varphi\Phi}v_\varphi^2 + \lambda_\Phi v_\Phi^2\Big) = 0,\end{aligned} \tag{13}$$

$$\begin{aligned}-\frac{\mu_1}{\sqrt{2}}v_\Phi^2 + 2\tilde{\lambda}_{\varphi\Phi}v_\varphi v_\Phi^2 + M_\varphi^2 v_\varphi + \frac{1}{2}\lambda_{\varphi H}v_\varphi v^2 \\ + \frac{1}{2}\lambda_{\varphi\Phi}v_\varphi v_\Phi^2 + \lambda_\varphi v_\varphi^3 = 0,\end{aligned} \tag{14}$$

$$v\left(-M_H^2 + \frac{1}{2}\lambda_{\varphi H}v_\varphi^2 + \frac{1}{2}\lambda_{\Phi H}v_\Phi^2 + \lambda_H v^2\right) = 0, \tag{15}$$

where the first, second, and third equations are obtained from $\partial V/\partial v_\Phi = 0$, $\partial V/\partial v_\varphi = 0$, and $\partial V/\partial v = 0$, respectively. In our analysis, we consider that the mixing among the SM Higgs and other scalar bosons are suppressed by assuming tiny values for $\lambda_{\varphi H}$ and $\lambda_{\Phi H}$, and the SM Higgs VEV is approximately given by $v \simeq \sqrt{M_H^2/\lambda_H}$ as in the SM; thus, $h$ is the SM-like Higgs boson. On the other hand, the VEVs $v_\varphi$ and $v_\Phi$ are determined by Eqs. (13) and (14) The VEVs obtained from these equations can be minimum of the potential. Here, we briefly discuss how we can realize the minimum of the potential when we take $M^2_{\{H,\chi,\varphi,\Phi\}} > 0$, $\lambda_{\{H,\varphi,\Phi,\chi\}} > 0$, $\lambda_{\{\varphi H,\Phi H,\varphi\Phi,\chi H,\chi\varphi,\chi\Phi\}} > 0$, and $\mu_1 > 0$. For $\mu_1 > 0$ case, nonzero values of $\langle\tilde{\Phi}_{\pm\pm}\rangle$ and $\langle\varphi_0\rangle$ provide negative contribution to the potential as we see from Eq. (10) and our vacuum configuration is preferred to obtain the minimum of the potential. We also assume small values for $\tilde{\lambda}_{\varphi\Phi}$ and $\mu_2$ so that the negative contributions to the potential from the corresponding terms do not affect the minimum of the potential. Note that a detailed analysis of the potential is difficult since we have many free parameters, and as such is beyond the scope of this paper. After spontaneous symmetry breaking, three degrees of freedom from $\Phi$ and $\varphi$ are absorbed by $SU(2)_D$ gauge bosons $\tilde{X}_\mu^{1,2,3}$, and the remaining scalar degrees of freedom from $\varphi$ and $\Phi$ become massive physical scalar bosons. Here, we do not discuss the details of these physical scalar bosons since they are irrelevant in our phenomenological analysis below.

Note that there is a remaining $Z_4$ symmetry in our scenario, where each $SU(2)_D$ multiplet $\xi$ transforms as $\xi \to e^{iT_3\pi}\xi$, with $T_3$ being the diagonal $SU(2)_D$ generator. We can understand the remnant $Z_4$ symmetry as follows. The quintet VEV $\langle\Phi\rangle$ is invariant under the unitary transformation of $U_{T_3} = e^{i\pi T_3}$, which is a part of $SU(2)_D$: $U_{T_3}\langle\Phi\rangle = \langle\Phi\rangle$, where $T_3 \equiv \mathrm{diag}(2,1,0,-1,-2)$ for the quintet (the triplet VEV $\langle\varphi\rangle$ has no effect since its $T_3$ value is 0). Then, a component $\xi_m$ in a multiplet $\xi$ transforms as $\xi_m \to e^{im\pi}\xi_m$,

where $m$ is the eigenvalue of $T_3$ for the component. Thus, a component with half-integer $m$ transforms as $\xi_m \to \pm i\xi$, while one with integer $m$ transforms as $\xi_m \to \pm\xi_m$. Therefore, we have the remaining $Z_4$ symmetry after spontaneous breaking of $SU(2)_D$. In our case, the components in the $SU(2)_D$ doublet have $Z_4$ charge $\pm i$, while the components of the triplet and quintet have charge $\pm 1$ or 0. As a result, $Z_4$ charged particles can be stable and become our DM candidates.

The scalar bosons from $\chi$ will be one of our DM candidates since they transform as $\chi_1(\chi_2) \to i\chi_1(-i\chi_2)$ under this remnant $Z_4$ symmetry. The mass matrix for $\chi$ is obtained as

$$\begin{pmatrix} \chi_1^* \\ \tilde{\chi}_2^* \end{pmatrix}^T \begin{pmatrix} \tilde{M}_\chi^2 & -\sqrt{2}\mu_2 v_\varphi \\ -\sqrt{2}\mu_2 v_\varphi & \tilde{M}_\chi^2 \end{pmatrix} \begin{pmatrix} \chi_1 \\ \tilde{\chi}_2 \end{pmatrix}, \quad (16)$$

where $\tilde{\chi}_2 \equiv \chi_2^*$ and $\tilde{M}_\chi^2 = M_\chi^2 + \frac{1}{2}\lambda_{\chi H} v^2 + \frac{1}{2}\lambda_{\chi\varphi} v_\varphi^2 + \frac{1}{2}\lambda_{\chi\Phi} v_\Phi^2$. We then obtain the mass eigenstates and eigenvalues such that

$$\begin{pmatrix} \chi_1 \\ \tilde{\chi}_2 \end{pmatrix}^T = \begin{pmatrix} \frac{1}{\sqrt{2}} & -\frac{1}{\sqrt{2}} \\ \frac{1}{\sqrt{2}} & \frac{1}{\sqrt{2}} \end{pmatrix} \begin{pmatrix} \rho_1 \\ \rho_2 \end{pmatrix}, \quad (17)$$

$$m_{1,2}^2 = \tilde{M}_\chi^2 \pm \sqrt{2}\mu_2 v_\varphi, \quad (18)$$

where we denote $m_{1,2}$ as the masses of $\rho_{1,2}$, choosing $m_1 < m_2$, and assume $\tilde{M}_\chi^2 > \sqrt{2}\mu_2 v_\varphi$ to make the eigenvalues positive.

### B. Gauge sector

Here we focus on the gauge sector of $SU(2)_L \times SU(2)_D \times U(1)_Y$, where the Lagrangian is

$$\mathcal{L}_G = -\frac{1}{4} W^{a\mu\nu} W^a_{\mu\nu} - \frac{1}{4} \tilde{X}^{\alpha\mu\nu} \tilde{X}^\alpha_{\mu\nu} - \frac{1}{4} \tilde{B}_{\mu\nu} \tilde{B}^{\mu\nu}, \quad (19)$$

and $W^{a\mu\nu}$ and $\tilde{B}^{\mu\nu}$ are the gauge field strengths of $SU(2)_L$ and $U(1)_Y$, respectively. In addition the terms in Eq. (19), a term connecting $SU(2)_D$ and $U(1)_B$ is generated by one-loop diagrams in which $L'$ propagates [25], as shown in Fig. 1. We obtain such a term as

$$\mathcal{L}_{XB} = \sum_a \frac{g_X g_B y_{aa}}{12\pi^2 M_{L'}} \tilde{B}_{\mu\nu} \tilde{X}^{\alpha\mu\nu} \varphi^\alpha. \quad (20)$$

Then. after $\varphi$ develops its VEV, we obtain the kinetic mixing term

$$\mathcal{L}_{KM} = \sum_a \frac{g_X g_B y_{aa} v_\varphi}{12\sqrt{2}\pi^2 M_{L'}} \tilde{B}_{\mu\nu} \tilde{X}^{3\mu\nu} \equiv -\frac{1}{2} \sin\zeta \tilde{B}_{\mu\nu} \tilde{X}^{3\mu\nu}, \quad (21)$$

where $\tilde{X}^3_{\mu\nu} \equiv \partial_\mu \tilde{X}^3_\nu - \partial_\nu \tilde{X}^3_\mu$. We thus find the magnitude of the kinetic mixing parameter $\sin\zeta$ as

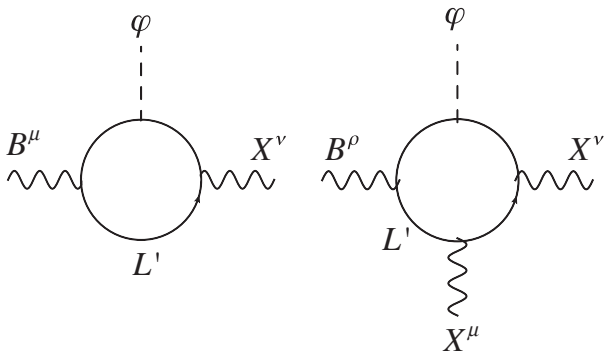


FIG. 1. One-loop diagrams generating kinetic mixing between $SU(2)_D$ and $U(1)_Y$.

$$\sin\zeta \simeq 1.8 \times 10^{-3} \frac{g_X}{0.5} \frac{v_\varphi}{M_{L'}} \sum_a y_{aa}. \quad (22)$$

In our analysis, we consider $\sin\zeta < 10^{-3}$. We can diagonalize the kinetic terms for $\tilde{X}^3_\mu$ and $\tilde{B}_\mu$ by using the following transformations:

$$\tilde{B}_\mu = B_\mu - \tan\zeta X^3_\mu, \quad (23)$$

$$\tilde{X}^3_\mu = \frac{1}{\cos\zeta} X^3_\mu. \quad (24)$$

Since the kinetic mixing term is generated at the one-loop level, $\zeta$ is typically very small. Thus, we can take $\tan\zeta \simeq \zeta$ and $\cos\zeta \simeq 1$, writing the gauge field approximately as

$$\tilde{B}_\mu \simeq B_\mu - \zeta X^3_\mu, \qquad \tilde{X}^3_\mu \simeq X^3_\mu. \quad (25)$$

After the quintet and triplet scalar fields develop nonzero VEVs, the mass terms for $SU(2)_D$ gauge fields and the SM $Z$ boson field are

$$L_M = \frac{1}{2} m^2_{Z_{\rm SM}} \tilde{Z}_\mu \tilde{Z} + m^2_{Z_{\rm SM}} \zeta \sin\theta_W \tilde{Z}_\mu X^{3\mu} + \frac{1}{2} m^2_{X^3} X^3_\mu X^{3\mu} + m^2_{X^\pm} X^+_\mu X^{-\mu}, \quad (26)$$

$$m^2_{Z_{\rm SM}} = \frac{v^2}{4}(g^2 + g_B^2), \qquad m^2_{X^3} = 4 g_X^2 v_\Phi^2,$$
$$m^2_{X^\pm} = g_X^2 v_\Phi^2 \left(1 + \frac{v_\varphi^2}{v_\Phi^2}\right), \quad (27)$$

where $g$ and $g_B$ are the gauge couplings of $SU(2)$ and $U(1)_Y$, $\tilde{Z}$ is the $Z$ boson field in the SM, and $X^\pm_\mu = (\tilde{X}^1_\mu \mp i\tilde{X}^2_\mu)/\sqrt{2}$. Diagonalizing the $\tilde{Z}$ and $X^3$ mass terms, we obtain the mass eigenstates and mixing angles as

$$m^2_{Z,Z'} = \frac{1}{2}(m^2_{X^3} + m^2_{Z_{\rm SM}}) \mp \frac{1}{2}\sqrt{(m^2_{X^3} - m^2_{Z_{\rm SM}})^2 + 4\zeta^2 \sin^2\theta_W m^4_{Z_{\rm SM}}}, \quad (28)$$

$$\tan 2\theta_{ZZ'} = \frac{2\sin\theta_W \zeta m^2_{Z_{\rm SM}}}{m^2_{Z_{\rm SM}} - m^2_{X^3}}, \quad (29)$$

where we approximate $m_Z \simeq m_{Z_{\rm SM}}$ and $m_{Z'} \simeq m_{X^3}$ for tiny $\zeta$, and we take $0 \le \theta_{ZZ'} \le \frac{\pi}{2}$ as our convention. Here, we emphasize that the mass relation $m_{Z'} \sim 2m_{X^\pm}$ is obtained when dark gauge boson masses are dominantly induced by the quintet VEV, and the $X^\pm$ annihilation cross section via $Z'$ is enhanced by resonant effect.

Thus, the mass eigenstates $Z$ and $Z'$ are written as

$$\begin{pmatrix} Z \\ Z' \end{pmatrix} = \begin{pmatrix} \cos\theta_{ZZ'} & -\sin\theta_{ZZ'} \\ \sin\theta_{ZZ'} & \cos\theta_{ZZ'} \end{pmatrix} \begin{pmatrix} \tilde{Z} \\ X^3 \end{pmatrix}. \quad (30)$$

We find that $\sin\theta_{ZZ'} \lesssim 10^{-4}$ for $\zeta \le 10^{-3}$ and $m_{X^\pm} \ge 100$ GeV. The $Z$-$Z'$ mixing modifies $Z$ interactions with the SM fermions, and electroweak precision tests should be considered. In fact, we can easily avoid current constraints from electroweak precision tests since $\theta_{ZZ'}$ is sufficiently small [29–31]. In addition, we can also avoid constraints from direct searches of $Z'$ boson at collider experiments since $Z'$ production cross section is small enough.

### C. Mass terms of hidden fermions

In this subsection we discuss mass terms for hidden fermions. *Neutral fermion masses:* After spontaneous symmetry breaking, we obtain mass terms of dark neutral fermions such that

$$\begin{aligned} L_{M_N} = {} & M_N^{ab}(\overline{n_1^a} n_1^b + \overline{n_2^a} n_2^b) + M_{nn}^{ab}(\overline{n_{2L}^{ca}} n_{1L}^b + \overline{n_{1L}^{ca}} n_{2L}^b) \\ & + \tilde{M}_{nn}^{ab}(\overline{n_{2R}^{ca}} n_{1R}^b + \overline{n_{1R}^{ca}} n_{2R}^b) + M_{D_n}^{ab}(\overline{n_{1L}^a} n_{1R}^b - \overline{n_{2L}^a} n_{2R}^b) \\ & + M_{nn'}^{ab}(n'^{\bar{a}}_{1R} n_{1L}^b + n'^{\bar{a}}_{2R} n_{2L}^b) \\ & + \tilde{M}_{nn'}^{ab}(n'^{\bar{a}}_{1L} n_{1R}^b + n'^{\bar{a}}_{2L} n_{2R}^b) \\ & + M_{L'}^{ab}(n'^{\bar{a}}_1 n'^b_1 + n'^{\bar{a}}_2 n'^b_2), \end{aligned} \quad (31)$$

where the mass matrices appearing in these terms are given by

$$M_{nn'}^{ab} = \frac{g_R^{ab}}{\sqrt{2}} v_H, \qquad \tilde{M}_{nn'}^{ab} = \frac{g_L^{ab}}{\sqrt{2}} v_H, \qquad M_{nn}^{ab} = \frac{y_{N_L}^{ab}}{2} v_\varphi,$$
$$\tilde{M}_{nn}^{ab} = \frac{y_{N_R}^{ab}}{2} v_\varphi, \qquad M_{D_n} = \frac{y_D^{ab}}{2} v_\varphi. \quad (32)$$

We thus obtain the Majorana mass matrix for dark neutral fermions under the basis $\Psi_R = (n'_{1R}, n'_{2R}, n'^c_{1L}, n'^c_{2L}, n_{1R}, n_{2R}, n^c_{1L}, n^c_{2L})^T$:

$$M_R = \begin{pmatrix} 0 & 0 & M_{L'}^T & 0 & 0 & 0 & M_{nn'}^* & 0 \\ 0 & 0 & 0 & M_{L'}^T & 0 & 0 & 0 & M_{nn'}^* \\ M_{L'} & 0 & 0 & 0 & \tilde{M}_{nn'} & 0 & 0 & 0 \\ 0 & M_{L'} & 0 & 0 & 0 & \tilde{M}_{nn'} & 0 & 0 \\ 0 & 0 & \tilde{M}_{nn'}^T & 0 & 0 & \tilde{M}_{nn}^\dagger & \tilde{M}_N^T + M_{D_n}^T & 0 \\ 0 & 0 & 0 & \tilde{M}_{nn'}^T & \tilde{M}_{nn}^\dagger & 0 & 0 & \tilde{M}_N^T - M_{D_n}^T \\ M_{nn'}^\dagger & 0 & 0 & 0 & \tilde{M}_N + M_{D_n} & 0 & 0 & M_{nn}^\dagger \\ 0 & M_{nn'}^\dagger & 0 & 0 & 0 & \tilde{M}_N - M_{D_n} & M_{nn}^\dagger & 0 \end{pmatrix}, \quad (33)$$

where indices that distinguish generations are omitted and it is $24 \times 24$ since each element is $3 \times 3$ matrix. This mass matrix can be diagonalized by the $24 \times 24$ orthogonal matrix $V_N$, assuming all matrix elements are real, and the mass eigenstates are given by

$$\psi_R = V_N^T \Psi_R. \quad (34)$$

We write the mass eigenvalues as $M_x (x = 1, \ldots, 24)$. The orthogonal matrix $V_N$ and mass $M_x$ can be obtained numerically.

*Charged fermion masses*: We obtain Dirac mass terms of $e'_{1,2}$ from the $M_{L'}\mathrm{Tr}[\bar{L}'L']$ term such that

$$M_{L'}\mathrm{Tr}[\bar{L}'L'] \supset M_{L'}(\overline{e'_1} e'_1 + \overline{e'_2} e'_2), \quad (35)$$

where index that distinguishes generation is omitted. We choose the basis in which $M_{L'}$ is diagonal without loss of generality.

## III. PHENOMENOLOGY

In this section we discuss the phenomenology of our model, such as active neutrino masses, LFVs, and DM physics.

### A. Neutrino mass generation and LFV

In this subsection we discuss the neutrino mass generation mechanism and related LFV processes. The relevant interactions are obtained from the first two terms of the third line on the rhs of Eq. (5). Writing the terms in terms of the mass eigenstates, we obtain

$$\begin{aligned}\mathcal{L} \supset & \frac{1}{\sqrt{2}} f^{+}_{ia} (V_N)_{ax} \overline{\nu^i_L} \psi^x_R \rho^*_1 + \frac{1}{\sqrt{2}} f^{-}_{ia} (V_N)_{ax} \overline{\nu^i_L} \psi^x_R \rho^*_2 \\ & - \frac{1}{\sqrt{2}} f^{-}_{ia} (V_N)_{3+a,x} \overline{\nu^i_L} \psi^x_R \rho_1 + \frac{1}{\sqrt{2}} f^{+}_{ia} (V_N)_{3+a,x} \overline{\nu^i_L} \psi^x_R \rho_2 \\ & + \frac{1}{\sqrt{2}} f^{+}_{ia} \overline{e^i_L} e'^a_{1R} \rho^*_1 + \frac{1}{\sqrt{2}} f^{-}_{ia} \overline{e^i_L} e'^a_{1R} \rho^*_2 - \frac{1}{\sqrt{2}} f^{-}_{ia} \overline{e^i_L} e'^a_{2R} \rho_1 + \frac{1}{\sqrt{2}} f^{+}_{ia} \overline{e^i_L} e'^a_{2R} \rho_2 + \text{H.c.}, \end{aligned} \tag{36}$$

where $f^{+}_{ia} = (f + f')_{ia}$ and $f^{-}_{ia} = (f - f')_{ia}$.

*Neutrino mass generation*: In our model, active neutrino masses are generated through the one-loop diagrams shown in Fig. 2, which are given by the original flavor eigenstates in the Lagrangian. The neutrino mass matrix is then calculated as

$$\begin{aligned}(M_\nu)_{ij} &= \frac{M_x}{(4\pi)^2} (f^{+}_{ia} f^{-}_{jb} m_1^2 - f^{-}_{ia} f^{+}_{jb} m_2^2) (V_N)_{ax} (V_N)_{3+b,x} \int_0^1 [dX]_3 \frac{1}{x M_x^2 + y m_1^2 + z m_2^2} + (i \leftrightarrow j) \\ &\simeq 10^{-10}\ \text{GeV} \frac{M_x}{\text{TeV}} \frac{(f^{+}_{ia} f^{-}_{jb} \frac{m_1^2}{m_2^2} - f^{-}_{ia} f^{+}_{jb}) (V_N)_{ax} (V_N)_{3+b,x}}{10^{-11}} \int_0^1 [dX]_3 \frac{m^2_{\rho_2}}{x M_x^2 + y m_1^2 + z m_2^2} \\ &\quad + (i \leftrightarrow j), \end{aligned} \tag{37}$$

where $\int_0^1 [dX]_3 = \int_0^1 dx dy dz \delta(1 - x - y - z)$ and summations over indices $\{a, b\}(= 1\text{–}3)$ and $x(= 1\text{–}24)$ are taken. It is possible to accommodate experimental data for the neutrino sector by tuning the Yukawa couplings $f^{\pm}_{ia}$, as we have 18 degrees of freedom (when Yukawa couplings are real). For illustration, we consider the current observed values of mixing angles and mass-squared differences in the normal-ordering case [32] (NuFit 5.0):

$$\begin{aligned}&\sin^2\theta_{12} = 0.304^{+0.013}_{-0.012}, \qquad \sin^2\theta_{23} = 0.570^{+0.018}_{-0.024}, \qquad \sin^2\theta_{13} = 0.02221^{+0.00068}_{-0.00062}, \\ &\Delta m^2_{\text{sol}} = 7.42^{+0.21}_{-0.20} \times 10^{-5}\ [\text{eV}^2], \qquad \Delta m^2_{\text{atm}} = 2.515^{+0.028}_{-0.027} \times 10^{-3}\ [\text{eV}^2], \end{aligned} \tag{38}$$

where $\Delta m^2_{\text{sol(atm)}}$ corresponds to the solar (atmospheric) mass-squared difference. In Table II we show a benchmark point that gives the observed mixing and mass-squared differences. For our benchmark point, we assume mass matrix $M_{L'}$, $M_N$, $M_{nn'}$, $\tilde{M}_{nn'}$, $M_{nn}$, $\tilde{M}_{nn}$ and $M_{D_n}$ to be diagonal for simplicity; nonzero elements of $V_N$ is found to be $\mathcal{O}(0.1)$ to $\mathcal{O}(1)$ and $M_x = \{M_1, \ldots, M_{24}\} \simeq \{80, \ldots, 1000\}$ GeV. We then obtain the mixing angles and mass-squared differences as outputs. The goodness of fit is evaluated by calculating the $\chi^2$ value,

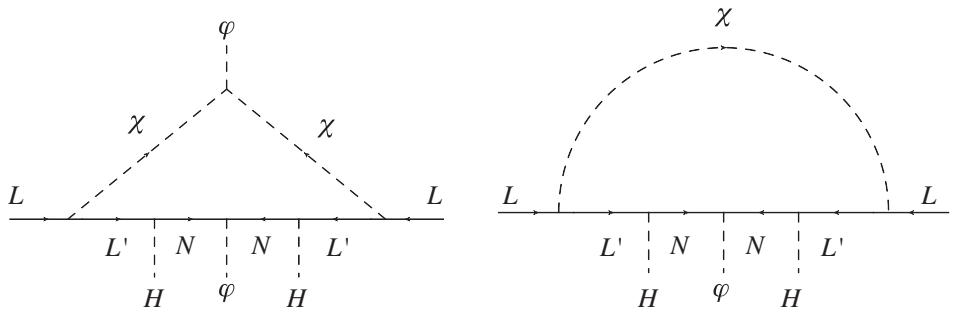


FIG. 2. One-loop diagrams generating neutrino masses.

TABLE II. Numerical benchmark point of our parameter sets and corresponding outputs.

| Input | |
|---|---|
| $M_N$ [GeV] | Diagonal [40, 50, 60] |
| $M_{L'}$ [GeV] | Diagonal [500, 700, 1000] |
| $M_{nn'}$ [GeV] | Diagonal [50, 70, 90] |
| $\tilde{M}_{nn'}$ [GeV] | Diagonal [60, 80, 100] |
| $M_{nn}$ [GeV] | Diagonal [100, 150, 180] |
| $\tilde{M}_{nn}$ [GeV] | Diagonal [110, 120, 130] |
| $\tilde{M}_{D_n}$ [GeV] | Diagonal [50, 70, 90] |
| $\{m_1, m_2\}$ [GeV] | $\{500, 800\}$ |
| $\{f^+_{11}, f^+_{12}, f^+_{13}, f^+_{21}, f^+_{22}, f^+_{23}, f^+_{31}, f^+_{32}, f^+_{33}\}$ | $\{1.82, 3.89, 3.16, -1.22, 4.45, 40.3, 4.81, 4.26, -10.7\} \times 10^{-7}$ |
| $\{f^-_{11}, f^-_{12}, f^-_{13}, f^-_{21}, f^-_{22}, f^-_{23}, f^-_{31}, f^-_{32}, f^-_{33}\}$ | $\{3.94, 7.73, -4.61, -4.71, 9.71, 21.5, -2.17, 85.3, -27.5\} \times 10^{-7}$ |
| Output | |
| $\sin^2\theta_{12}$ | 0.300 |
| $\sin^2\theta_{23}$ | 0.557 |
| $\sin^2\theta_{13}$ | 0.0214 |
| $\Delta m^2_{\rm sol}$ | $7.56 \times 10^5$ eV$^2$ |
| $\Delta m^2_{\rm atm}$ | $2.53 \times 10^3$ eV$^2$ |
| $\chi^2$ | 2.66 |

$$\chi^2 = \sum_i \left( \frac{O_i^{\rm th} - O_i^{\rm exp}}{\sigma_i} \right)^2, \tag{39}$$

where $O^{\rm th}$, $O^{\rm exp}$, and $\sigma$ are the theoretically obtained value, experimentally observed value, and experimental error for the observables in Eq. (38). Note that we did not consider $CP$ phase choosing real Yukawa couplings for simplicity; but it is easy to add complex phases in coupling and obtain $CP$ phase in the neutrino mass matrix.

*LFV decays of charged leptons*: Yukawa interactions associated with charged dark fermions induce LFV decay of $\ell \to \ell'\gamma$ at the one-loop level. We then estimate the BRs by calculating relevant one-loop diagrams, and the branching ratio of $\ell_i \to \ell_j \gamma$ is given by

$$B(\ell_i \to \ell_j \gamma) = \frac{48\pi^3 C_{ij} \alpha_{\rm em}}{G_F^2 m_i^2} (|(a_R)_{ij}|^2 + |(a_L)_{ij}|^2), \tag{40}$$

where $m_{i(j)}$, $(i(j) = 1, 2, 3)$ is the mass for the initial (final) state of the charged lepton identified as $1 \equiv e, 2 \equiv \mu, 3 \equiv \tau$, and $(C_{21}, C_{31}, C_{32}) = (1, 0.1784, 0.1736)$. Relevant amplitudes are estimated as

$$\begin{aligned}(a_R)_{ij} = &-\sum_{K=1,2} \frac{f^+_{ja} f^{+\dagger}_{ai}}{2(4\pi)^2} m_{\ell_j} \int_0^a [dX]_3 \frac{xz}{x(x-1)m^2_{\ell_i} + xm^2_K + (y+z)m^2_{e'^a_K}} \\ &- \frac{f^-_{ja} f^{-\dagger}_{ai}}{2(4\pi)^2} m_{\ell_j} \int_0^a [dX]_3 \frac{xz}{x(x-1)m^2_{\ell_i} + xm^2_2 + (y+z)m^2_{e'^a_1}} \\ &- \frac{f^-_{ja} f^{-\dagger}_{ai}}{2(4\pi)^2} m_{\ell_j} \int_0^a [dX]_3 \frac{xz}{x(x-1)m^2_{\ell_i} + xm^2_1 + (y+z)m^2_{e'^a_2}},\end{aligned} \tag{41}$$

$$\begin{aligned}(a_L)_{ij} = &-\sum_{K=1,2} \frac{f^+_{ja} f^{+\dagger}_{ai}}{2(4\pi)^2} m_{\ell_i} \int_0^a [dX]_3 \frac{xy}{x(x-1)m^2_{\ell_i} + xm^2_K + (y+z)m^2_{e'^a_K}} \\ &- \frac{f^-_{ja} f^{-\dagger}_{ai}}{2(4\pi)^2} m_{\ell_i} \int_0^a [dX]_3 \frac{xy}{x(x-1)m^2_{\ell_i} + xm^2_2 + (y+z)m^2_{e'^a_1}} \\ &- \frac{f^-_{ja} f^{-\dagger}_{ai}}{2(4\pi)^2} m_{\ell_i} \int_0^a [dX]_3 \frac{xy}{x(x-1)m^2_{\ell_i} + xm^2_1 + (y+z)m^2_{e'^a_2}}.\end{aligned} \tag{42}$$

The current experimental upper bounds for the BRs are given by [33–35]

$$B(\mu \to e\gamma) \le 4.2 \times 10^{-13}, \qquad B(\tau \to \mu\gamma) \le 4.4 \times 10^{-8},$$
$$B(\tau \to e\gamma) \le 3.3 \times 10^{-8}. \tag{43}$$

We can easily avoid these constraints at our benchmark point since the Yukawa coupling $f_{ia}^{\pm}$ tends to be smaller than $\mathcal{O}(10^{-5})$ and the LFV decay ratios are much smaller than current constraints.

### B. Dark matter

In our model DM candidates are $Z_4$ charged particles in the dark sector, which are $X^{\pm}$, $\rho_{1,2}$, $\varphi^{\pm}$, and $\psi_R^x$. Here, we consider a scenario in which $\rho_{1,2}$ and/or $X^{\pm}$ are DM candidates choosing the other particles to be heavier than them. Under $Z_4$ symmetry, $\rho_{1,2}$ and $X^{\pm}$ transform as $\rho_{1,2} \to i\rho_{1,2}$ and $X^{\pm} \to -X^{\pm}$, respectively. In our analysis we focus on gauge interactions to calculate relic density of DM candidates since scalar portal interaction is preferred to be small to avoid constraints from direct-detection experiments of DM, and Yukawa couplings $f_{ia}$ should be very small to realize neutrino mass as we discussed above.

First, interactions among dark gauge bosons are written as

$$\mathcal{L} \supset -g_X \epsilon^{\alpha\beta\gamma} \partial_\mu \tilde{X}_\nu^\alpha \tilde{X}^{\beta\mu} \tilde{X}^{\gamma\nu} - \frac{1}{4} g_X^2 \epsilon^{\alpha\beta\gamma} \epsilon^{\alpha\rho\sigma} \tilde{X}_\mu^\beta \tilde{X}_\nu^\gamma \tilde{X}^{\sigma\mu} \tilde{X}^{\rho\nu}, \tag{44}$$

where $\epsilon^{\alpha\beta\gamma}$ are the structure constants of $SU(2)_D$. We note that the four-point gauge interaction in Eq. (44) does not provide the dominant contribution to the DM annihilation process since $m_{Z'} \simeq m_{X^3} \gtrsim m_{X^{\pm}}$ in our scenario. Thus, we focus on the three-point interactions which are written in terms of mass eigenstates $X^{\pm}$ and $Z'$ as

$$\mathcal{L} \supset i g_X C_{ZZ'} [(\partial_\mu X_\nu^+ - \partial_\nu X_\mu^+) X^{-\mu} Z'^\nu - (\partial_\mu X_\nu^- - \partial_\nu X_\mu^-) X^{+\mu} Z'^\nu + \frac{1}{2} (\partial_\mu Z'_\nu - \partial_\nu Z'_\mu)(X^{+\mu} X^{-\nu} - X^{-\mu} X^{+\nu})], \tag{45}$$

where $C_{ZZ'} \equiv \cos\theta_{ZZ'}$. Through the $Z$-$Z'$ mixing, $Z'$ interactions with SM fermions $f$ are obtained as

$$\mathcal{L}_{Z'\bar{f}f} = \sum_{X=L,R} \frac{g}{\cos\theta_W} Z'_\mu \bar{f}_X \gamma^\mu [S_{ZZ'}(T_3 - Q_f \sin^2\theta_W) + C_{ZZ'} \zeta Y \sin\theta_W] f_X, \tag{46}$$

where $T_3$ is the diagonal generator of $SU(2)_L$, $Q_f$ is the electric charge of an SM fermion, and $S_{ZZ'} \equiv \sin\theta_{ZZ'}$. Gauge interactions associated with scalar DM candidates $\rho_{1,2}$ are also obtained as

$$\mathcal{L} \supset i \frac{g_X C_{ZZ'}}{2} Z'_\mu (\rho_1^* \partial^\mu \rho_1 - \rho_1 \partial^\mu \rho_1^* + \rho_2^* \partial^\mu \rho_2 - \rho_2 \partial^\mu \rho_2^*) + i \frac{g_X}{\sqrt{2}} X_\mu^+ (\rho_1^* \partial^\mu \rho_2^* - \rho_2^* \partial^\mu \rho_1^*) - i \frac{g_X}{\sqrt{2}} X_\mu^- (\rho_1 \partial^\mu \rho_2 - \rho_2 \partial^\mu \rho_1) + \frac{g_X^2}{4} C_{ZZ'}^2 Z'_\mu Z'^\mu (\rho_1^* \rho_1 + \rho_2^* \rho_2) - \frac{g_X^2}{2} (X_\mu^+ Z'^\mu \rho_1^* \rho_2^* + X_\mu^- Z'^\mu \rho_1 \rho_2). \tag{47}$$

Note that our DM candidates can also interact with the SM $Z$ boson through the mixing effect. These are obtained by substituting $\{C_{ZZ'}, Z'_\mu\}$ for $\{S_{ZZ'}, Z_\mu\}$. Such interactions are thus suppressed by the tiny $S_{ZZ'}$ in our scenario.

In our scenario we have more than one DM component, depending on the mass relations among $X^{\pm}$, $\rho_1$, and $\rho_2$:

(1) $m_{X^{\pm}} + m_1 < m_2 \to X^{\pm}$ and $\rho_1$ are DM.
(2) $m_1 + m_2 < m_{X^{\pm}} \to \rho_1$ and $\rho_2$ are DM.
(3) $m_2 - m_1 < m_{X^{\pm}} < m_1 + m_2 \to \rho_1$, $\rho_2$ and $X^{\pm}$ are DM.

Here $\rho_2$ decays into $\rho_1^* X_+$ in case 1, while $X^{\pm}$ decays into $\rho_1^{(*)} \rho_2^{(*)}$ in case 2. In the following, we consider case 1; in case 2, the scalar portal interaction tends to be required as dark gauge bosons are heavier, and case 3 is more complicated as we have three DM components. The relevant DM annihilation processes in case 1 are given by the diagrams in Fig. 3: pair annihilation of $\rho_{1,2}$, pair annihilation of $X^{\pm}$, the semiannihilation $\rho_{1(2)}\rho_{1(2)} \to X^+ Z'$, and the semi-coannihilation $\rho_1 \rho_2 \to X^+ Z'$ ($Z'$ decays into SM particles). Then, we scan the relevant parameters $\{m_{X^{\pm}}, m_1, g_X\}$ within the following regions:

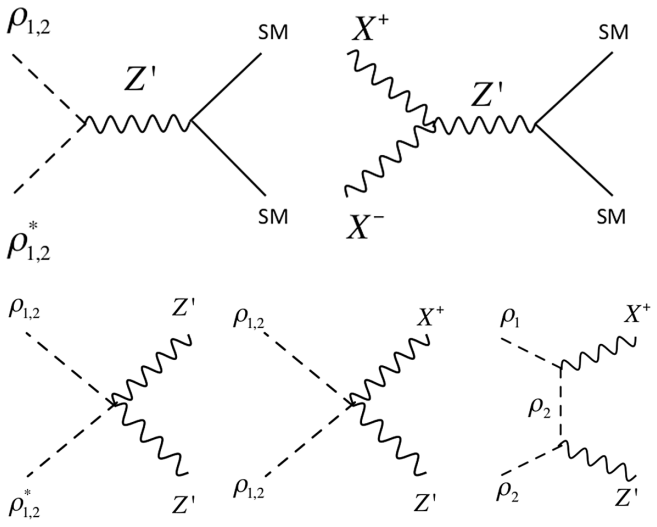


FIG. 3. Feynman diagrams for DM annihilation processes.

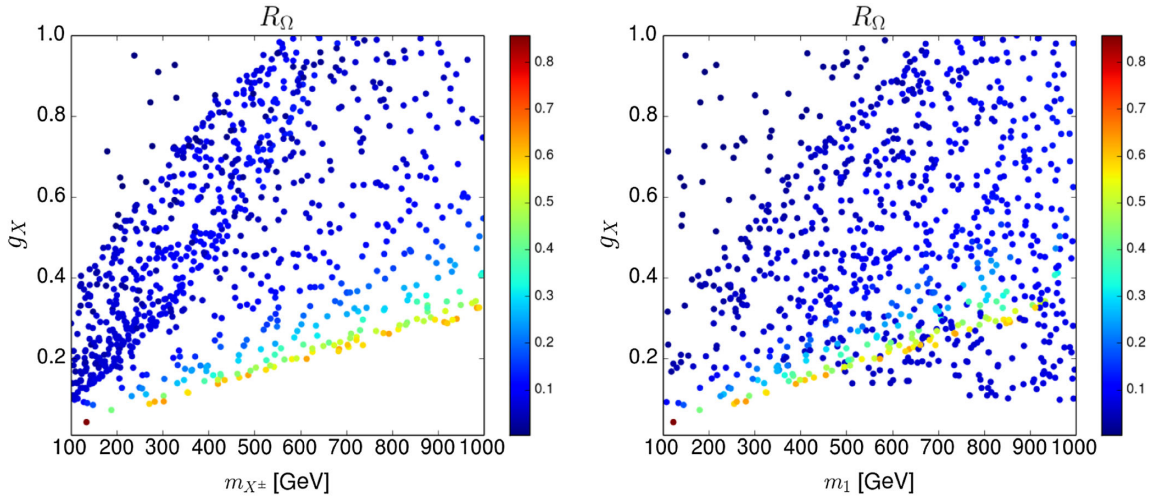


FIG. 4. Parameter points satisfying the observed relic density, where the color gradient indicates the ratio of the relic density $R_\Omega \equiv \Omega_{X^\pm}/\Omega_{\rho_1}$. For the left and right panels, the horizontal axis corresponds to the mass of $X^\pm$ and $\rho_1$, respectively.

$$m_{X^\pm} \in [100, 1000]\ \text{GeV}, \qquad m_1 \in [100, 1000]\ \text{GeV},$$
$$g_X \in [0.01, 1.0], \tag{48}$$

where we fix the other parameters as $m_2 = m_{X^\pm} + m_1 + 100$ GeV, $v_\varphi^2/v_\Phi^2 = 0.1$, and $\zeta = 5 \times 10^{-4}$. We then estimate the relic density of $\rho_1$ and $X^\pm$, where we use micrOMEGAs 5 [36] to implement relevant interactions. In the left and right panels of Fig. 4, we show parameter points in the $\{m_{X^\pm}, g_x\}$ and $\{m_1, g_x\}$ planes satisfying the observed relic density in the approximated region $0.11 < \Omega h^2 = (\Omega_{X^\pm} + \Omega_{\rho_1})h^2 < 0.13$ around $\Omega h^2 \simeq 0.12$ [37], where the color gradient indicates the ratio of the relic density for two DM components: $R_\Omega \equiv \Omega_{X^\pm}/\Omega_{\rho_1}$. In addition, we show the parameter points realizing the observed relic density in the $\{m_{X^\pm}, m_1\}$ plane in Fig. 5. We find that the relic density of $X^\pm$ tends to be smaller than that of $\rho_1$ since the cross section of the $X^\pm X^\pm \to Z' \to f_{\rm SM} f_{\rm SM}$ process is enhanced by the resonant condition $m_{Z'} \sim 2m_{X^\pm}$. The relic density of the two components can be of similar order when $m_{X^\pm} \sim m_1 \sim m_{Z'}/2$. Note also that the relic density can be explained in the region where $\rho_1$ is much heavier than $X^\pm$. In this region, $\rho_{1(2)}$ can annihilate into dark gauge bosons, including semiannihilation and semi-coannihilation processes, and the relic density of $\rho_1$ can be reduced to satisfy $\Omega h^2 \sim 0.12$. Note that we can also choose a larger ratio $v_\varphi^2/v_\Phi^2$ by modifying parameters in the scalar potential. In that case, the mass relation between $X^\pm$ and $Z'$ does not satisfy resonant condition $m_{Z'} \sim 2m_{X^\pm}$ and the relic density of $X^\pm$ will be larger for fixed $g_X$; $R_\Omega$ in Figs. 4 and 5 becomes larger for larger $v_\varphi/v_\Phi$.

Here we comment on constraints from the direct detection of our DM candidates. Our DM can interact with nucleons via $Z'$ and $Z$ boson exchange processes associated with $Z$-$Z'$ mixing. In our model, the mixing is small since it is induced at the loop level and the DM-nucleon scattering cross section will be sufficiently small to avoid current constraints. For example, we can estimate the cross section for $\rho_1$-nucleon scattering[1] as

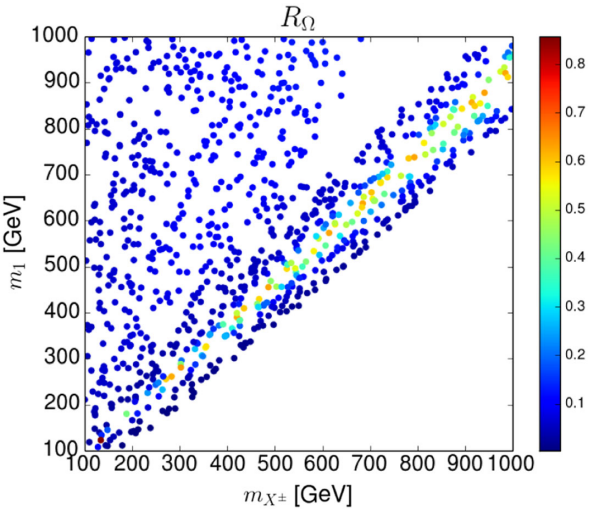


FIG. 5. Parameter points satisfying the observed relic density in the two-DM mass plane, where the color gradient is the same as in Fig. 4.

$$\sigma_{p[n]-\rho_1} \simeq \frac{g_X^2 e^2 \zeta^2}{2\pi \cos^2\theta_W} \left(\frac{19}{36}\left[\frac{1}{4}\right]\right) \frac{m_{p[n]}^2}{m_{Z'}^4}$$
$$\sim g_X^2 \left(\frac{\zeta}{10^{-4}}\right)^2 \left(\frac{200\ \text{GeV}}{m_{Z'}}\right)^4 10^{-46}\ \text{cm}^2, \tag{49}$$

[1]The $X^\pm$-DM scattering cross section tends to be smaller than that of $\rho_1$.

where $p[n]$ stands for proton[neutron]. Thus, our parameter region is safe from constraints of DM direct detections [37,38] when the kinetic mixing is sufficiently small.

## IV. SUMMARY AND DISCUSSION

We have discussed a model based on dark $SU(2)_D$ gauge symmetry in which we introduced $SU(2)_L \times SU(2)_D$ bidoublet vector-like leptons. The bidoublets connect the dark sector and SM sector through the interaction associated with the SM lepton doublets and $SU(2)_D$ scalar doublet. Then, we obtained active neutrino masses and interactions realizing kinetic mixing between $SU(2)_D$ and $U(1)_Y$ gauge fields at the loop level. Moreover, there is a remnant $Z_4$ symmetry after the spontaneous breaking of $SU(2)_D$ in our scenario, and this symmetry guarantees the stability of our DM candidates.

We have formulated the active neutrino mass matrix and related LFV processes in our model. Also, the relic density of our DM candidates was estimated by scanning some relevant parameters. Remarkably, we found a multicomponent scenario in some parameter space where we have vector and scalar DM components. We have shown the parameter points realizing the observed relic density, where vector DM tends to provide a smaller relic density due to the resonant enhancement of the corresponding annihilation cross section.

## ACKNOWLEDGMENTS

This research was supported by an appointment to the Junior Research Group (JRG) Program at the Asia Pacific Center for Theoretical Physics (APCTP) through the Science and Technology Promotion Fund and Lottery Fund of the Korean Government. It was also supported by the Korean Local Governments—Gyeongsangbuk-do Province and Pohang City (H. O.). H. O. is sincerely grateful for the KIAS member.

## APPENDIX: SOME FORMULAS FOR THE $SU(2)_D$ QUINTET

Here we summarize some formulas to write interactions for the $SU(2)_D$ quintet. We write $SU(2)_D$ generators in $5 \times 5$ form (denoted by $\mathcal{T}_a^{(5)}$) such that

$$\mathcal{T}_1^{(5)} = \frac{1}{2}\begin{pmatrix} 0 & 2 & 0 & 0 & 0 \\ 2 & 0 & \sqrt{6} & 0 & 0 \\ 0 & \sqrt{6} & 0 & \sqrt{6} & 0 \\ 0 & 0 & \sqrt{6} & 0 & 2 \\ 0 & 0 & 0 & 2 & 0 \end{pmatrix},$$

$$\mathcal{T}_2^{(5)} = \frac{i}{2}\begin{pmatrix} 0 & -2 & 0 & 0 & 0 \\ 2 & 0 & -\sqrt{6} & 0 & 0 \\ 0 & \sqrt{6} & 0 & -\sqrt{6} & 0 \\ 0 & 0 & \sqrt{6} & 0 & -2 \\ 0 & 0 & 0 & 2 & 0 \end{pmatrix},$$

$$\mathcal{T}_3^{(5)} = \mathrm{diag}(2, 1, 0, -1, -2). \tag{A1}$$

We can then write $SU(2)_D$ gauge interactions for the quintet $\Phi$ using the kinetic term $(D_\mu \Phi)^\dagger (D^\mu \Phi)$, where the covariant derivative is

$$D_\mu \Phi = (\partial_\mu + i g_X \mathcal{T}_a^{(5)} X_\mu^a)\Phi_5. \tag{A2}$$

[1] P. Ko, J. Korean Phys. Soc. **73**, 449 (2018).
[2] L. M. Krauss and F. Wilczek, Phys. Rev. Lett. **62**, 1221 (1989).
[3] C. W. Chiang, T. Nomura, and J. Tandean, J. High Energy Phys. 01 (2014) 183.
[4] C. H. Chen and T. Nomura, Phys. Lett. B **746**, 351 (2015).
[5] C. H. Chen and T. Nomura, Phys. Rev. D **93**, 074019 (2016).
[6] C. H. Chen, C. W. Chiang, and T. Nomura, Phys. Lett. B **747**, 495 (2015).
[7] C. H. Chen, C. W. Chiang, and T. Nomura, Phys. Rev. D **97**, 061302 (2018).
[8] T. Nomura, H. Okada, and S. Yun, J. High Energy Phys. 06 (2021) 122.
[9] P. Ko, T. Nomura, and H. Okada, Phys. Rev. D **103**, 095011 (2021).
[10] C. Gross, O. Lebedev, and Y. Mambrini, J. High Energy Phys. 08 (2015) 158.
[11] T. Hambye, J. High Energy Phys. 01 (2009) 028.
[12] C. Boehm, M. J. Dolan, and C. McCabe, Phys. Rev. D **90**, 023531 (2014).
[13] N. Baouche, A. Ahriche, G. Faisel, and S. Nasri, Phys. Rev. D **104**, 075022 (2021).
[14] S. Baek, P. Ko, and W. I. Park, J. Cosmol. Astropart. Phys. 10 (2014) 067.
[15] V. V. Khoze and G. Ro, J. High Energy Phys. 10 (2014) 061.
[16] R. Daido, S. Y. Ho, and F. Takahashi, J. High Energy Phys. 01 (2020) 185.

[17] H. Davoudiasl and I. M. Lewis, Phys. Rev. D **89**, 055026 (2014).
[18] B. Barman, S. Bhattacharya, S. K. Patra, and J. Chakrabortty, J. Cosmol. Astropart. Phys. 12 (2017) 021.
[19] B. Barman, S. Bhattacharya, and M. Zakeri, J. Cosmol. Astropart. Phys. 09 (2018) 023.
[20] B. Barman, S. Bhattacharya, and M. Zakeri, J. Cosmol. Astropart. Phys. 02 (2020) 029.
[21] B. Barman, S. Bhattacharya, and B. Grzadkowski, J. High Energy Phys. 12 (2020) 162.
[22] A. Karam and K. Tamvakis, Phys. Rev. D **92**, 075010 (2015).
[23] E. Hall, T. Konstandin, R. McGehee, H. Murayama, and G. Servant, J. High Energy Phys. 04 (2020) 042.
[24] T. Ghosh, H. K. Guo, T. Han, and H. Liu, J. High Energy Phys. 07 (2021) 045.
[25] T. Nomura and H. Okada, Phys. Lett. B **821**, 136630 (2021).
[26] H. Okada and K. Yagyu, Phys. Rev. D **89**, 053008 (2014).
[27] H. Okada, T. Toma, and K. Yagyu, Phys. Rev. D **90**, 095005 (2014).
[28] H. Okada and Y. Orikasa, Phys. Rev. D **94**, 055002 (2016).
[29] P. Langacker, Rev. Mod. Phys. **81**, 1199 (2009).
[30] V. V. Andreev, P. Osland, and A. A. Pankov, Phys. Rev. D **90**, 055025 (2014).
[31] T. Bandyopadhyay, G. Bhattacharyya, D. Das, and A. Raychaudhuri, Phys. Rev. D **98**, 035027 (2018).
[32] I. Esteban, M. C. Gonzalez-Garcia, A. Hernandez-Cabezudo, M. Maltoni, and T. Schwetz, J. High Energy Phys. 01 (2019) 106.
[33] B. Aubert *et al.* (*BABAR* Collaboration), Phys. Rev. Lett. **104**, 021802 (2010).
[34] A. M. Baldini *et al.* (MEG Collaboration), Eur. Phys. J. C **76**, 434 (2016).
[35] F. Renga (MEG Collaboration), Hyperfine Interact. **239**, 58 (2018).
[36] G. Belanger, F. Boudjema, A. Pukhov, and A. Semenov, Comput. Phys. Commun. **192**, 322 (2015).
[37] P. A. Zyla *et al.* (Particle Data Group), Prog. Theor. Exp. Phys. **2020**, 083C01 (2020).
[38] E. Aprile *et al.* (XENON Collaboration), Phys. Rev. Lett. **121**, 111302 (2018).